

Time-resolved *in situ* measurement of mitochondrial malfunction by energy transfer spectroscopy

Herbert Schneckenburger

Institut für Lasertechnologien in der Medizin
und Messtechnik an der Universität Ulm
Ulm, Germany,
Institut für Angewandte Forschung
Fachhochschule Aalen
Aalen, Germany

Michael H. Gschwend

Universität Ulm, Abteilung für Allgemeine Physiologie
Ulm, Germany

Reinhard Sailer

Institut für Lasertechnologien in der Medizin
und Messtechnik an der Universität Ulm
Ulm, Germany

Wolfgang S. L. Strauss

Institut für Lasertechnologien in der Medizin
und Messtechnik an der Universität Ulm
Ulm, Germany

Marco Lyttek

Institut für Angewandte Forschung
Fachhochschule Aalen
Aalen, Germany

Karl Stock

Institut für Lasertechnologien in der Medizin
und Messtechnik an der Universität Ulm
Ulm, Germany
Institut für Angewandte Forschung
Fachhochschule Aalen
Aalen, Germany

Peter Zipfl

Institut für Angewandte Forschung
Fachhochschule Aalen
Aalen, Germany

1 Introduction

An increasing number of diseases such as mitochondrial myopathies,^{1–4} neurodegenerative diseases,^{4,5} and impairments of energy metabolism by environmental toxins⁶ or drugs⁷ have been related to malfunction of the mitochondrial respiratory chain. Detection and characterization of mitochondrial malfunction often require complex biochemical procedures after cell lysis. In contrast, fluorometric methods are nondestructive and may be suitable for detecting specific metabolites in living cells or tissues. In particular, intrinsic fluorescence of the coenzyme nicotinamide adenine dinucleotide in its reduced form (NADH)^{8–10} has so far been examined. Fluorescence intensity of NADH has been proposed to be an appropriate parameter for detection of ischemic^{11,12} or neoplastic^{13–15} tissues. Fluorescence spectra of NADH exhibit two overlapping emission bands with maxima around 440 nm

Abstract. To establish optical *in situ* detection of mitochondrial malfunction, nonradiative energy transfer from the coenzyme NADH to the mitochondrial marker rhodamine 123 (R123) was examined. Dual excitation of R123 via energy transfer from excited NADH molecules as well as by direct absorption of light results in two fluorescence signals whose ratio is a measure of mitochondrial NADH. A screening system was developed in which these signals are detected simultaneously using a time-gated (nanosecond) technique for energy transfer measurements and a frequency selective technique for direct excitation and fluorescence monitoring of R123. Optical and electronic components of the apparatus are described, and results obtained from cultivated endothelial cells are reported. The ratio of fluorescence intensities excited in the near ultraviolet and blue–green spectral ranges increased by a factor 1.5 or 1.35 after inhibition of the mitochondrial respiratory chain by rotenone at cytotoxic or noncytotoxic concentrations, respectively. Concomitantly the amount of mitochondrial NADH increased. Excellent linearity between the number of cells incubated with R123 and fluorescence intensity was found in suspension. © 2000 Society of Photo-Optical Instrumentation Engineers. [S1083-3668(00)00504-9]

Keywords: mitochondrial malfunction, mitochondrial NADH, rhodamine 123, energy transfer, time-resolved fluorescence screening.

Paper JBO-90057 received Nov. 1, 1999; revised manuscript received Apr. 11, 2000 and June 26, 2000; accepted for publication June 26, 2000.

for the extended conformation and 465 nm for the folded conformation of the molecule. The extended conformation occurs when NADH is bound to proteins, whereas the folded conformation is found for unbound (“free”) NADH. Previously, using time-resolved fluorescence spectroscopy, malfunctioning of the respiratory chain has been correlated with fluorescence intensity of free NADH.^{10,16}

In living cells, fluorescence of mitochondrial NADH is commonly superposed by the fluorescence of cytoplasmic NADH as well as by nicotinamide adenine dinucleotide phosphate (NADPH) with almost identical emission spectra. Therefore, in order to detect mitochondrial NADH selectively, nonradiative energy transfer from NADH (the energy donor) to the mitochondrial marker rhodamine 123 (Ref. 17) (R123; the energy acceptor) has been examined.¹⁶ If energy transfer according to the Förster mechanism should exceed spontaneous deactivation of the donor, intermolecular distances of less than 10 nm are required.¹⁸ A further prerequisite of this resonant energy transfer mechanism is an overlap of

Address all correspondence to Prof. Herbert Schneckenburger, Fachhochschule Aalen, Institut für Angewandte Forschung, Postfach 1728, D-73428 Aalen, Germany. Tel: +49-7361-568-229 or -49-7361-568-0; Fax: +49-7361-568-225; E-mail: herbert.schneckenburger@fh-aalen.de

the emission spectrum of the donor with the absorption spectrum of the acceptor. Spectral overlap of the emission of free NADH and absorption of R123 (maximum around 495 nm) is sufficiently fulfilled. However, R123 is a membrane potential probe, and its accumulation is expected to depend on mitochondrial membrane potential. Since the fluorescence quantum yield of R123 is about 0.9 compared with 0.02 for free NADH,¹⁹ energy transfer from mitochondrial NADH to R123 is detected with high sensitivity.

As described previously,¹⁶ excitation of the coenzyme NADH with subsequent nonradiative energy transfer to R123 molecules induces a fluorescence signal of R123 whose intensity is linearly related to both donor (NADH) and acceptor (R123) concentrations. When using direct optical excitation of R123, its fluorescence intensity is proportional to the intracellular amount of R123, if the concentration within the incubation medium is below 25 μM . Therefore, the ratio of both fluorescence signals is linearly related to donor concentration and appears to be a measure of mitochondrial NADH, since all other parameters of this ratio (e.g., the concentration-independent energy transfer rate, extinction coefficients as well as the fluorescence quantum yield of the acceptor) are expected to remain unchanged. Previous measurements using fluorescence microscopy¹⁶ showed an increase of this ratio up to a factor of 4 after inhibition of specific enzyme complexes of the mitochondrial respiratory chain. At present, microscopic detection has been replaced by *in situ* measurements, using 96 well dishes. This permits rapid screening of samples with rather small statistical variances when large numbers of cells per sample are examined. For simultaneous measurement of R123 using indirect (via energy transfer) as well as direct excitation, two different detection modes are required. Therefore, the apparatus presently described includes (1) excitation of NADH in the near ultraviolet region by nanosecond laser pulses and time-gated detection of R123 fluorescence and (2) continuous excitation of R123 by a frequency modulated light emitting diode in the blue-green spectral range and frequency selective detection of R123 fluorescence.

2 Materials and Methods

In vitro experiments of BKEz-7 endothelial cells from calf aorta²⁰ were carried out within black 96 well dishes (Optiplate II; Deelux, G6denstorf, Germany). Cells were routinely cultivated in Eagle's minimum essential medium (MEM) supplemented with 10% fetal calf serum (FCS), glutamine (2 mM), and antibiotics (penicillin, streptomycin) at 37°C and 5% CO₂. Part of the experiments was carried out with almost confluent growing monolayers, which were obtained after a growth period of 36 h when 500 cells mm⁻² were seeded. After this growth period the medium was removed, and cells were incubated for 30 min with R123 at concentrations of 1, 5, 10, 15, or 25 μM . According to a proliferation test as well as an MTT test (probing the activity of mitochondrial dehydrogenases) these concentrations were noncytotoxic.^{16,21} In addition, the amount of intracellular adenosine triphosphate (ATP) remained almost constant upon incubation with the highest concentration of R123 (25 μM),²¹ similar to reports on isolated mitochondria.²² However, according to further reports in the literature,²³ especially in combination with irradiation during fluorescence measurements,²² some inhibition

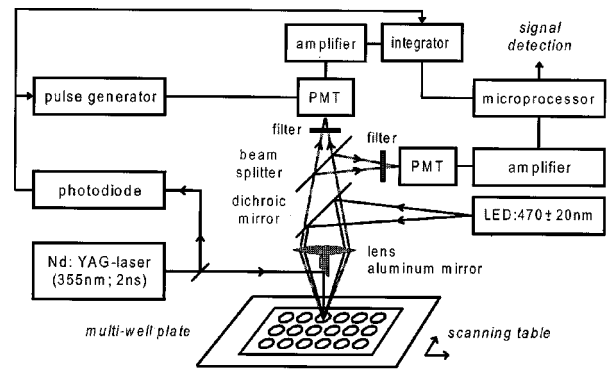


Fig. 1 Optical and electronic setup for energy transfer measurements *in situ* using time-gated and frequency selective fluorescence detection. Excitation wavelengths: 355 nm (pulsed laser) or 470±20 nm (modulated LED); emission measured at $\lambda \geq 515$ nm.

of mitochondrial metabolism cannot be excluded. At the end of the incubation period, the medium was removed, and cells were rinsed twice with phosphate buffered saline (PBS) (at 37°C) and covered with 100 μL PBS prior to fluorometric measurements. In addition, cells were coincubated for 30 min with R123 (10 μM) and rotenone, a well-known inhibitor of the first enzyme complex of the mitochondrial respiratory chain,²⁴ at a concentration of 1 μM or 25 nM. According to both MTT and proliferation assays,²¹ the first concentration of rotenone was cytotoxic towards BKEz-7 endothelial cells, showing about 50% survival (IC₅₀) 48 h after incubation, whereas the latter one was noncytotoxic with more than 90% survival after 48 h. Further experiments were carried out with suspensions of BKEz-7 endothelial cells at well defined cell numbers between 1.56×10^4 and 2.5×10^5 . For this, cells growing within cultivation flasks were incubated for 30 min with R123 (25 μM in MEM), washed three times with PBS, detached (with 1 mL trypsin/EDTA), centrifuged, and counted in a Neubauer chamber, described elsewhere.¹⁶ Cellular suspensions were further diluted with PBS, and 100 μL samples were used for fluorescence measurements. Integral light doses during measurements were below 0.4 J/cm² and revealed to be nonphototoxic towards BKEz-7 endothelial cells incubated with R123 (see Ref. 16).

As shown in Figure 1, 96 well dishes are moved on a scanning table by an *x, y* step motor. Individual samples are placed within the beams of a pulsed Nd:YAG laser (DCR 11; Spectra Physics, Mountain View, CA; $\lambda=355$ nm, pulse duration 2.5 ns, pulse energy 500 μJ , repetition rate 10 Hz) as well as a frequency modulated light emitting diode (LED) (2 mW; modulation frequency 1083 Hz) equipped with an interference filter for 470±20 nm. LED radiation is deflected and focused onto the sample using a dichroic mirror (510 nm) and a 25 mm biconvex lens, whereas laser radiation is deflected onto the sample by a highly reflecting aluminum mirror of 5 mm diameter. The beam diameters of focused LED and divergent laser radiation are both adapted to the diameter of the samples (6 mm). Fluorescence light is collimated by a lens ($f=25$ mm; same as above), split into two detection paths, and detected by two photomultiplier tubes (PMTs) after transmission of 515 nm long pass filters. Alternatively, interference filters for 530±20 nm (corresponding to the emission

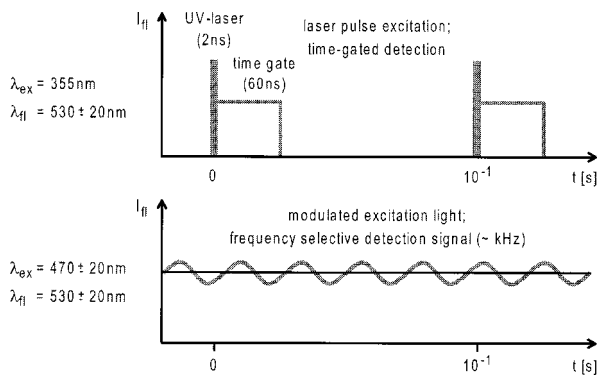


Fig. 2 Simultaneous time-gated and frequency selective detection of rhodamine 123 fluorescence after laser pulse or modulated LED excitation.

maximum of R123) can be used. The electric signal of the first photomultiplier (9318; Hamamatsu Photonics; Figure 1, right) is fed to a frequency selective amplifier (1083 Hz), which is synchronized with the LED using lock-in techniques. The second photomultiplier (R6427; Hamamatsu Photonics; Figure 1, top) is operated in a time-gated mode. The first three dynodes of this photomultiplier are in a short circuit except from periods of 60 ns when a square wave of about 300 V amplitude is generated by discharge of a coaxial transmission line, resulting in voltages of 100 V between adjacent dynodes.²⁵ The pulse generator is triggered optically by the laser pulses using a fast photodiode with an amplifier and pulse shaper, such that the time gate is opened about 5 ns after the onset of the laser pulse. The output signal of the photomultiplier is again amplified and integrated over a period of 80 ns, which is slightly longer than the time gate of the photomultiplier. Although the selected time gate is long as compared with the fluorescence lifetime of R123,¹⁶ it permits suppression of long-lived (microsecond) ultraviolet (UV)-induced parasitic luminescence of the experimental setup.

Time-gated and frequency selective detection modes are depicted in Figure 2. Laser-induced fluorescence is detected within time gates of 60 ns prior to “dark times” of almost 100 ms each. Therefore, superposition by continuous LED-induced fluorescence becomes negligible. On the other hand, the frequency selective fluorescence signal induced by LED is only slightly affected by laser-induced fluorescence. In order to suppress laser-induced background completely, frequency selective detection is turned off during the short durations of aperture of the time gate. These different operation modes permit simultaneous detection of R123 fluorescence after energy transfer from NADH and after direct optical excitation. The ratio of both signals is calculated in a microprocessor and is a measure of mitochondrial NADH. The microprocessor also records variations of the pulse energy of the Nd:YAG laser as well as drifts of LED power, and allows correction of the measured signals.

3 Results

The fluorescence intensity of monolayers of BKEz-7 endothelial cells incubated with various concentrations of R123 (1–25 μ M) showed a monotonous increase with concentration for both excitation wavelengths, 355 and 470 ± 20 nm,

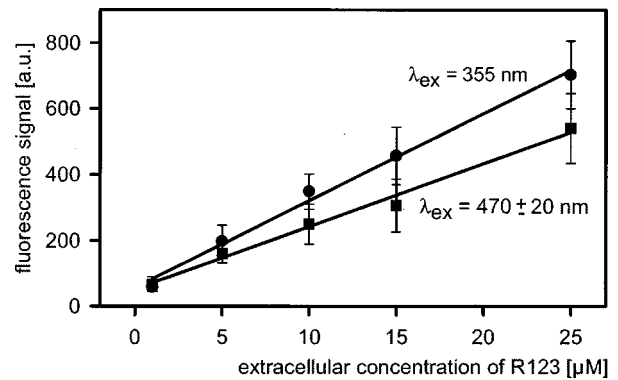


Fig. 3 Fluorescence signal of almost confluent monolayers of BKEz-7 endothelial cells after incubation with various concentrations of R123 using either laser pulse excitation (355 nm) and time-gated detection, or modulated excitation (470 ± 20 nm) and frequency selective detection; emission measured at $\lambda \geq 515$ nm. Median \pm MAD (median absolute deviation) of eight measurements in each case.

used for time-gated or frequency selective measurements, respectively. In both cases, the fluorescent background (cells covered by 100 μ L PBS) was about 75% of the signal measured for the smallest concentration of 1 μ M R123 and proved to be reproducible within $\pm 5\%$. After subtraction of this background, a linear relationship between fluorescence intensity and extracellular concentration of R123 was found for both excitation wavelengths between 1 and 25 μ M (Figure 3). Standard deviations of the fluorescence intensity were about $\pm 15\%$, i.e., considerably smaller than in previous microscopic experiments,^{16,26} but similar to variations of the intracellular amount of R123.¹⁶ Background luminescence at $\lambda \geq 515$ nm was assigned to autofluorescence (mainly of flavin molecules^{9,27,28}), superimposed by some parasitic luminescence of the optical components, in particular the multiwell dishes.

Measurements of suspensions of BKEz-7 endothelial cells incubated with 25 μ M R123 showed excellent linearity between the fluorescence intensity and the cell number with standard deviations below $\pm 10\%$ for time-gated as well as for frequency selective detection (Figure 4). The contribution of autofluorescence of the cells (and the optical components) de-

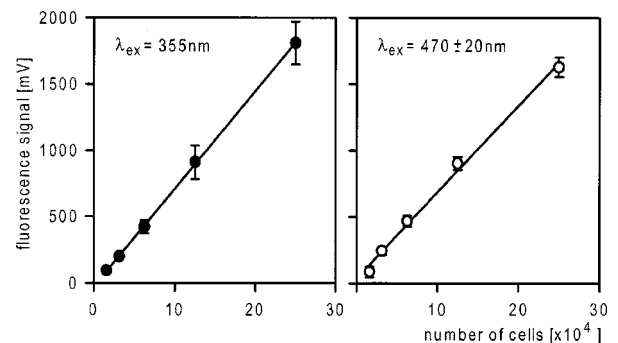


Fig. 4 Fluorescence signal of R123 at various numbers of BKEz-7 endothelial cells in suspension using laser pulse excitation (355 nm) and time-gated detection (left) or modulated excitation (470 ± 20 nm) and frequency selective detection (right); emission measured at $\lambda \geq 515$ nm. Mean \pm standard deviation of 10 measurements in each case.

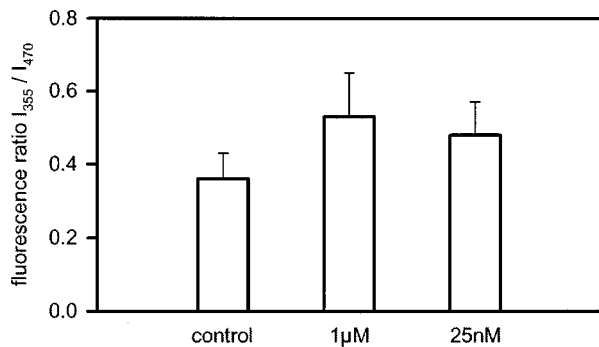


Fig. 5 Fluorescence ratio I_{355}/I_{470} of BKEz-7 endothelial cells from calf aorta after incubation with R123 (10 μ M; control) or coincubation with R123 (10 μ M) and rotenone at cytotoxic (1 μ M) or noncytotoxic (25 nM) concentration. Excitation wavelengths: 355 nm (pulsed laser) and 470 ± 20 nm (modulated LED); emission measured at $\lambda \geq 515$ nm. Mean \pm standard deviation of 40 measurements in each case.

creased from about 20% for the smallest cell number (1.56×10^4) to less than 5% for the largest cell number (2.5×10^5). No deviation from linearity due to light scattering was observed. Therefore, in addition to adherent cells, the method appears to be appropriate for quantitative fluorescence measurements of cellular suspensions.

For energy transfer measurements of mitochondrial malfunction, monolayers of BKEz-7 endothelial cells were incubated with R123 (10 μ M; control) or coincubated with R123 (10 μ M) and rotenone at cytotoxic (1 μ M) or noncytotoxic (25 nM) concentrations. Ratios of fluorescence intensities were calculated after excitation at 355 nm (time-gated detection) and 470 ± 20 nm (frequency selective detection). Results of 40 measurements in each case (given in arbitrary units) are depicted in Figure 5. Figure 5 shows an increase of the fluorescence ratio I_{355}/I_{470} by a factor of 1.5 after addition of 1 μ M rotenone or by a factor of 1.35 after addition of 25 nM rotenone which is concomitant with an increase of mitochondrial NADH.

4 Discussion

A novel fluorescence screening system for selective detection of mitochondrial NADH *in situ* is described. *In situ* measurement of mitochondrial malfunction has great potential, e.g., for detection of mitochondrial myopathies, neurodegenerative diseases, or impairments of energy metabolism by environmental toxins or drugs.¹⁻⁷ In addition, the impact of certain pharmaceuticals (e.g., cytostatics,²⁹ neuroleptics,³⁰ or sedatives³¹) on mitochondrial metabolism may be examined. Following inhibition of the mitochondrial respiratory chain, a pronounced increase of mitochondrial NADH (assessed as an increase of the fluorescence ratio I_{355}/I_{470}) was detected *in situ* for cytotoxic as well as for noncytotoxic concentrations of the inhibitor rotenone, thus proving the high sensitivity of the method. The increase of the fluorescence ratio I_{355}/I_{470} measured *in situ* after inhibition of the mitochondrial respiratory chain was larger than the increase of NADH fluorescence in microscopic experiments¹⁶ and comparable to bioluminescence measurements of intracellular NADH after cell lysis and extraction. In the latter case the amount of NADH in-

creased by a factor of 1.7 after application of 1 μ M rotenone³² or by a factor of 1.35 after application of 25 nM rotenone (unpublished data).

Previous microscopic experiments on energy transfer spectroscopy of cultivated BKEz-7 endothelial cells showed an increase of mitochondrial NADH by a factor of around 4 after inhibition of the first enzyme complex by rotenone (1 μ M) and of a factor of 1.8 after inhibition of the third enzyme complex of the respiratory chain by antimycin (5 μ M).¹⁶ Standard deviations of values obtained from small collectives of about five individual cells in each case were over $\pm 50\%$ compared with $\pm 15\%$ for the large cell collectives in multiwell dishes. A smaller increase of mitochondrial NADH upon inhibition of the respiratory chain was thus detected within the multiwell dishes as compared to the fluorescence microscope. In the latter case, experiments were performed under visual control, i.e., cells with a pronounced mitochondrial pattern of R123 fluorescence were selected, whereas in multiwell experiments some overlap by a diffuse fluorescent background occurred. This background fluorescence included smaller amounts of cytoplasmic R123 as well as some larger amounts of extracellular R123, which was attached to the multiwell dishes. Improvement in washing the microtiter plates and future work with cell suspensions (which are incubated with R123 in separate vials) will permit reduction of background fluorescence arising from the multiwell dishes. Furthermore, an enhancement of the sensitivity in the detection of mitochondrial NADH should be pursued as a goal. For this the fluorescent marker (energy acceptor) should be highly specific for the mitochondria. Due to the small standard deviations, detection of mitochondrial NADH in multiwell dishes appears to be more reliable than fluorescence microscopy in view of future routine applications.

A linear relationship between the number of cells incubated with R123 and fluorescence intensity was observed in suspensions despite pronounced light scattering. Therefore, it appears promising to carry out energy transfer measurements with nonadherent cells, e.g., lymphocytes or platelets. Reduced enzyme activities of the respiratory chain were observed within platelets of patients suffering from Parkinson's,³³ Huntington's³⁴ or Alzheimer's³⁵ disease. Therefore, fluorescence screening of platelets may support the diagnosis of neurodegenerative diseases. In the future, the actual screening time of 5–10 min for a 96 well plate can be shortened, or screening can even be replaced by simultaneous detection of a larger number of samples using time-gated imaging techniques.

Acknowledgments

The authors thank A. Schuh, L. Schoch, A. Hendinger, and C. Hintze for their cooperation. Financial support by the Bundesministerium für Bildung und Forschung (BMBF) under Grant No. 1705997 is gratefully acknowledged.

References

1. S. DiMauro, E. Bonilla, M. Zeviani, M. Nakagawa, and D. C. DeVivo, "Mitochondrial myopathies," *Ann. Neurol.* **17**, 521–526 (1985).
2. R. A. Capaldi, "Mitochondrial myopathies and respiratory chain proteins," *Trends Biochem. Sci.* **13**, 144–148 (1988).

3. D. C. Wallace, "Diseases of the mitochondrial DNA," *Annu. Rev. Biochem.* **61**, 1175–1212 (1992).
4. R. Luft, "The development of mitochondrial medicine," *Proc. Natl. Acad. Sci. U.S.A.* **91**, 8731–8738 (1994).
5. A. H. V. Schapira, "Evidence for mitochondrial dysfunction in Parkinson's disease—A critical appraisal," *Mov. Disord.* **9**, 125–138 (1994).
6. P. R. Smith, J. M. Cooper, G. G. Govan, E. A. Harding, and A. H. V. Schapira, "Smoking and mitochondrial function: A model for environmental toxins," *Q. J. Med.* **86**, 657–660 (1993).
7. C. Yuan and D. Acosta, Jr., "Cocaine-induced mitochondrial dysfunction in primary cultures of rat cardiomyocytes," *Toxicology* **112**, 1–10 (1996).
8. T. Galeotti, G. D. V. van Rossum, D. H. Mayer, and B. Chance, "On the fluorescence of NAD(P)H in whole cell preparations of tumours and normal tissues," *Eur. J. Biochem.* **17**, 485–496 (1970).
9. J.-M. Salmon, E. Kohen, P. Viallet, J. G. Hirschberg, A. W. Wouters, C. Kohen, and B. Thorell, "Microspectrofluorometric approach to the study of free/bound NAD(P)H ratio as metabolic indicator in various cell types," *Photochem. Photobiol.* **36**, 585–593 (1982).
10. R.-J. Paul and H. Schneckenburger, "Oxygen concentration and the oxidation-reduction state of yeast: Determination of free/bound NADH and flavins by time-resolved spectroscopy," *Naturwissenschaften* **83**, 32–35 (1996).
11. K. A. Horvath, D. F. Torchiana, W. M. Daggett, and N. S. Nishioka, "Monitoring myocardial reperfusion injury with NADH fluorometry," *Lasers Surg. Med.* **12**, 2–6 (1992).
12. E. T. Obi-Tabot, L. M. Hanrahan, R. Cachecho, E. R. Berr, S. R. Hopkins, J. C. K. Chan, J. M. Shapiro, and W. W. LaMorte, "Changes in hepatocyte NADH fluorescence during prolonged hypoxia," *J. Surg. Res.* **55**, 575–580 (1993).
13. W. Lohmann and E. Paul, "In situ detection of melanomas by fluorescence measurements," *Naturwissenschaften* **75**, 201–202 (1988).
14. M. Anidjar, O. Cussenot, S. Avriplier, D. Etori, J. M. Villette, J. Fiet, P. Teillac, and A. LeDuc, "Ultraviolet laser-induced autofluorescence distinction between malignant and normal urothelial cells and tissues," *J. Biomed. Opt.* **1**, 335–341 (1996).
15. B. Banerjee, B. Miedema, and H. R. Chandrasekhar, "Emission spectra of colonic tissue and endogenous fluorophores," *Am. J. Med.* **315**, 220–226 (1998).
16. H. Schneckenburger, M. H. Gschwend, W. S. L. Strauss, R. Sailer, M. Kron, U. Steeb, and R. Steiner, "Energy transfer spectroscopy for measuring mitochondrial metabolism in living cells," *Photochem. Photobiol.* **66**, 34–41 (1997).
17. L. V. Johnson, M. L. Walsh, and L. B. Chen, "Localization of mitochondria in living cells with rhodamine 123," *Proc. Natl. Acad. Sci. U.S.A.* **77**, 990–994 (1980).
18. T. Förster, "Zwischenmolekularer Übergang von Elektronen-anregungsenergie," *Z. Elektrochem.* **64**, 157–165 (1960).
19. T. G. Scott, R. D. Spencer, N. J. Leonard, and G. Weber, "Emission properties of NADH. Studies of fluorescence lifetimes and quantum efficiencies of NADH, AcPyADH, and simplified synthetic models," *J. Am. Chem. Soc.* **92**, 687–695 (1970).
20. W. Halle, W.-E. Siems, K. D. Jentsch, E. Teuscher, and E. Görres, "Die in vitro kultivierte Aorten-Endothelzelle in der Wirkstoffforschung—Zellphysiologische Charakterisierung und ein- satzmöglichkeiten der Zelllinie BKEz-7," *Die Pharmazie* **39**, 77–81 (1984).
21. M. H. Gschwend, "Untersuchungen mitochondrialer Funktionsstö- rungen an Zellkulturen mittels mikroskopischer Energietransferspek- troskopie," Doctoral thesis, Universität Ulm, 1998.
22. A. Atlante, S. Passarella, G. Moreno, and P. Salet, "Effects of rhodamine 123 in the dark and after irradiation on mitochondrial energy metabolism," *Photochem. Photobiol.* **56**, 471–478 (1992).
23. J. L. Vargas, E. Roche, E. Knecht, F. Aniento, and S. Grisolia, "The mitochondrial probe rhodamine 123 inhibits in isolated hepatocytes the degradation of short-lived proteins," *FEBS Lett.* **233**, 259–262 (1988).
24. A. Tzagaloff, *Mitochondria*, Plenum, New York (1982).
25. P. Zipfl, H. Schneckenburger, and L. Schoch, "Fast photomultiplier tube gating technique for time-resolved fluorescence measurements," in *Biomedical Imaging: Reporters, Dyes and Instrumentation*, D. J. Bornhop, C. H. Contag, and E. Sevick-Muraca, Eds., *Proc. SPIE* **3600**, 158–164 (1999).
26. H. Schneckenburger, M. H. Gschwend, W. S. L. Strauss, R. Sailer, M. Bauer, and R. Steiner, "Time-resolved energy transfer spectroscopy for measuring mitochondrial metabolism in living cells," in *Optical Biopsy and Microscopic Techniques II*, I. J. Bigio, H. Schneckenburger, J. Slavik, K. Svanberg, P. Viallet, Eds., *Proc. SPIE* **3197**, 160–167 (1997).
27. M. Nokubo, I. Zs.-Nagy, K. Kitani, and M. Ohta, "Characterization of the autofluorescence of rat liver plasma membranes," *Biochim. Biophys. Acta* **939**, 441–448 (1988).
28. P. Galland and H. Senger, "The role of flavins as photoreceptors," *J. Photochem. Photobiol., B* **1**, 277–294 (1988).
29. B. B. Hasinoff, "Inhibition and inactivation of NADH-cytochrome *c* reductase activity of bovine heart submitochondrial particles by the iron (III)-adriamycin complex," *Biochem. J.* **265**, 865–870 (1990).
30. J. A. Prince, M. S. Yassin, and L. Orelund, "Neuroleptic-induced mitochondrial enzyme alterations in the rat brain," *J. Pharmacol. Exp. Ther.* **280**, 261–267 (1997).
31. M. Colleoni, B. Costa, E. Gori, and A. Santagostino, "Biochemical characterization of the effects of the benzodiazepine, midazolam, on mitochondrial electron transfer," *Pharmacol. Toxicol.* **78**, 69–76 (1996).
32. H. Schneckenburger, M. H. Gschwend, R. Sailer, H.-P. Mock, and W. S. L. Strauss, "Time-gated fluorescence microscopy in cellular and molecular biology," *Cell. Mol. Biol.* **44**, 795–805 (1998).
33. D. Krige, M. T. Carroll, J. M. Cooper, C. D. Marsden, and A. H. V. Schapira, "Platelet mitochondrial function in Parkinson's disease," *Ann. Neurol.* **32**, 782–788 (1992).
34. W. D. Parker, Jr., S. J. Boyson, A. S. Luder, and J. K. Parks, "Evi- dence for a defect in NADH: Ubiquinone oxidoreductase (complex I) in Huntington's disease," *Neurology* **40**, 1230–1234 (1990).
35. W. D. Parker, Jr., N. J. Mahr, C. M. Filley, J. K. Parks, D. Hughes, D. A. Young, and C. M. Cullum, "Reduced platelet cytochrome *c* oxi- dase activity in Alzheimer's disease," *Neurology* **44**, 1086–1090 (1994).